

000 001 002 003 004 005 006 007 008 009 010 011 012 013 014 015 016 017 018 019 020 021 022 023 024 025 026 027 028 029 030 031 032 033 034 035 036 037 038 039 040 041 042 043 044 045 046 047 048 049 050 051 052 053 DTO-KD: DYNAMIC TRADE-OFF OPTIMIZATION FOR EFFECTIVE KNOWLEDGE DISTILLATION

Anonymous authors

Paper under double-blind review

ABSTRACT

Knowledge Distillation (KD) is a widely adopted framework for compressing large models into compact student models by transferring knowledge from a high-capacity teacher. Despite its success, KD presents two persistent challenges: (1) the trade-off between optimizing for the primary task loss and mimicking the teacher’s outputs, and (2) the gradient disparity arising from architectural and representational mismatches between teacher and student models. In this work, we propose Dynamic Trade-off Optimization for Knowledge Distillation (DTO-KD), a principled multi-objective optimization formulation of KD that dynamically balances task and distillation losses at the gradient level. Specifically, DTO-KD resolves two critical issues in gradient-based KD optimization: (i) gradient conflict, where task and distillation gradients are directionally misaligned, and (ii) gradient dominance, where one objective suppresses learning progress on the other. Our method adapts per-iteration trade-offs by leveraging gradient projection techniques to ensure balanced and constructive updates. We evaluate DTO-KD on large-scale benchmarks including ImageNet-1K for classification and COCO for object detection. Across both tasks, DTO-KD outperforms prior KD methods, yielding state-of-the-art accuracy and improved convergence behavior. Furthermore, student models trained with DTO-KD exceed the performance of their non-distilled counterparts, demonstrating the efficacy of our multi-objective formulation for KD. [The source code and models will be released upon acceptance.](#)

1 INTRODUCTION

Large deep learning models have achieved remarkable success in computer vision tasks, but their adoption is often limited by high computational costs, making it challenging to deploy on resource-constrained systems like edge devices and mobile phones. To address this, there has been a growing interest in reducing model size while maintaining performance. One effective approach achieving this is so called *knowledge distillation* (KD) (Yim, 2017; Gao et al., 2018; Qiu et al., 2023; Zhou et al., 2020), where a smaller model, called the student, is trained to mimic the outputs of a larger, pre-trained model, known as the teacher. This technique allows the student model to learn from the teacher’s knowledge, enabling it to achieve competitive performance with fewer parameters, making it more suitable for deployment on devices with limited resources. In a typical KD pipeline, this process involves a task-specific loss function, such as classification or object detection, alongside a mechanism to transfer knowledge from the teacher to the student.

Earlier works in KD (Hinton et al., 2015; Zhang et al., 2018) focused on using the teacher’s predictions as the ground-truth for the student model. However, this approach has limitations, as the teacher’s output is often overly compressed, and distilling knowledge solely from the final logits restricts the amount of useful information that can be transferred. To address this, later KD techniques (Romero et al., 2015; Chen et al., 2020; Heo et al., 2019a) shifted toward distilling knowledge from the teacher’s feature space, enabling a more flexible and informative transfer process. This is typically achieved by heuristic design choices and additional hyperparameters that need task-specific tuning. Despite advancements, feature-based KD approaches (Chen et al., 2022; 2021; Roy Miles & Deng, 2024) still struggle with effectively transferring knowledge from complex teacher models to simpler student models due to the inconsistency between the optimization objectives of ground-truth supervision and the distillation targets.

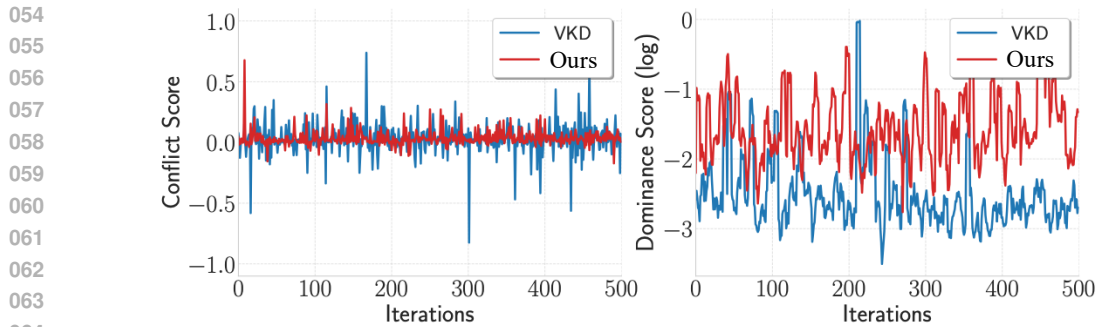


Figure 1: **Gradient Dynamics analysis**, comparing the conflict and dominance behavior of the distillation and task gradients. **Left**) Conflict score is computed as $\langle \mathbf{g}_{\text{dist}}, \mathbf{g}_{\text{task}} \rangle$, where more negative values indicate stronger disagreement. **Right**) Dominance score is calculated as $\frac{|\mathbf{g}_{\text{dist}}|}{|\mathbf{g}_{\text{task}}|}$ and shown in log-scale, with lower values indicating stronger dominance. DTO-KD achieves lower gradient conflict and more balanced gradient dominance compared to the baseline.

The optimization inconsistency is a key factor limiting the efficiency of teacher mimicking (Wang et al., 2024; Chen et al., 2022; Wang et al., 2024; Lin, 1976) approaches. The primary issue limiting the performance of these approaches is two-fold. First, **Gradient Conflicts (GrC)** arise when the gradients of the task-specific objective and the distillation process are misaligned. Second, **Gradient Dominance (GrD)** occurs when the gradient magnitude of one objective (e.g., either distillation or task-specific) dominates the learning process, causing an imbalance. Figure 1 illustrates these issues by plotting gradient conflict (GrC) and gradient dominance (GrD) for our method and that of Roy Miles & Deng (2024) over 500 iterations on the object detection task.

To address all of these issues, we propose a novel distillation optimization strategy. Specifically, we frame the problem as a dynamic trade-off optimization, which not only efficiently resolves gradient conflicts during training but also ensures a Pareto optimal (Lin, 1976) solution. This results in a training strategy that eliminates the need for manually tuning hyperparameters to balance the contributions of each loss function. Instead, it dynamically learns the contribution of each loss function, adapting between task-specific and distillation-specific objectives throughout the training.

To be more specific, in this paper we propose a closed-form method for determining how to weight the distillation and task-specific losses during training. Unlike the prior work of (Liu et al., 2023), our approach provides an explicit solution that can be computed efficiently at each step. In teacher-student architectures, where the distillation and task losses evolve rapidly, existing task-weighting methods (Hu et al., 2024; Zheng & Yang, 2024) can struggle to adapt, causing weights to oscillate or lag behind the changing dynamics. In contrast, our closed-form solution produces an update direction that is jointly aligned with both objectives, ensuring that neither the distillation nor the task loss dominates or interferes with the other. As a result, our method naturally mitigates gradient conflict and yields a more stable and effective multi-objective learning process.

In this paper, we introduce DTO-KD (Dynamic Trade-off Optimization for Knowledge Distillation), a novel multi-objective learning framework that formulates knowledge distillation as a gradient-level optimization problem. DTO-KD improves the efficiency and effectiveness of knowledge transfer by dynamically modulating the contribution of task-specific and distillation-specific objectives during training, removing the need for manual loss weighting or extensive hyperparameter tuning. DTO-KD is trained end to end and demonstrates faster convergence, requiring fewer epochs to reach or exceed the performance of state-of-the-art distillation methods.

In summary, the contributions of this paper are as follows:

- We propose DTO-KD, a dynamic trade-off optimization framework that balances task and distillation losses at the gradient level. This principled approach eliminates the need for fixed loss weighting, enabling adaptive trade-offs during training.
- DTO-KD resolves gradient conflict (GrC) and dominance (GrD) via per-iteration gradient balancing approach, leading to aligned, balanced updates and improved convergence.

108 • We conduct extensive experiments on both classification and detection benchmarks, achieving
 109 state-of-the-art performance. Ablation studies confirm the robustness of DTO-KD
 110 across diverse distillation setups.

111
 112 **2 RELATED WORK**
 113

114 This section explores KD techniques, focusing on the use of logits, CNN features, and transformer
 115 features (or tokens). Additionally, it examines multi-objective approaches relevant to the DTO-KD.

116 **Logit-based knowledge distillation:** Logit-based techniques have traditionally emphasized the dis-
 117 tillation process by utilizing solely the output logits. For instance, Zhang et al. (2018) uses an en-
 118 semble of students who learn collaboratively, while Mirzadeh et al. (2020) employs a multi-stage
 119 distillation with a teacher assistant network. Additionally, Zhao et al. (2022a) introduces a decou-
 120pling strategy, applying distillation to different branches of the teacher’s output individually. **Most**
 121 **logit-based methods use forward KL-divergence to align student and teacher distributions, which can**
 122 **over-smooth, whereas reverse KL-divergence (Wang et al., 2025a) focuses on the teacher’s domi-**
 123 **nant modes. Recently, Wang et al. (2025b) generalizes this with an α - β -divergence that interpolates**
 124 **between the two.** However, the logit-based distillation has key limitations: it transfers only the final
 125 layer’s outputs, missing rich feature representations from earlier layers, and limits the student’s abil-
 126 ity to generalize and learn deeper knowledge. The student model also struggles to align the teacher’s
 127 context-specific predictions with the task-specific objectives, leading to suboptimal learning.

128 **Feature-based knowledge distillation:** Feature-based KD focuses on utilizing intermediate layer
 129 features to relay knowledge from the teacher to the student model (Yang et al., 2021; Xu et al., 2020).
 130 Firstly, introduced in Romero et al. (2015), as a stage-wise training approach, where the student
 131 network is first trained up to a specific layer and then gradually distills the knowledge from the
 132 teacher. Building on this, Heo et al. (2019a) uses margin ReLU to filter redundant features, aligning
 133 transformed features, positions, and distances between teacher and student to improve knowledge
 134 transfer efficiency. Chen et al. (2021) investigates the connection paths between different levels
 135 of the teacher and student networks, highlighting their crucial role in enhancing the distillation
 136 process. Additionally, a diffusion model-based method (Huang et al., 2024) reduces the noise in
 137 student models before distilling the knowledge from a teacher. Furthermore, Wang et al (2024)
 138 introduces a new norm and direction loss function alongside the KD loss. However, feature-based
 139 distillation approaches are limited in transferring knowledge as they struggle to capture long-range
 140 dependencies and global context, which are crucial for understanding the teacher’s latent space.

141 **Token-based knowledge distillation:** Touvron et al. (2022) introduced the first convolution-free
 142 transformer for object classification, using token distillation for the student to learn from the teacher
 143 via attention. Song et al. (2021; 2022) proposed token-matching distillation for detection, where the
 144 student mimics the teacher’s tokens, but simple token-mimicking is suboptimal. To improve this,
 145 Ren et al. (2022) formulated multi-teacher distillation with lightweight teachers co-advising the stu-
 146 dent, and Hao et al. (2022) adapted a manifold-based approach for fine-grained token alignment.
 147 **Recently, Wen et al. (2023) formulates distillation using generalized f-divergences, emphasizing**
 148 **dominant teacher predictions while allowing flexible weighting across tokens.** Despite these, trans-
 149 ferring dark knowledge remains challenging. Yang et al. (2023) applied normalization to non-target
 150 logits and explored self-distillation, while Chen et al. (2022) proposed a two-stage method with
 151 early-layer distillation followed by standard training. These methods are ad hoc; in this paper, we
 152 propose an end-to-end strategy using dynamic trade-off optimization.

153 **Multi-objective optimization:** Multi-objective optimization (MOO) enables simultaneous opti-
 154 mization of conflicting objectives by seeking Pareto-optimal trade-offs. A simple approach re-
 155 weights loss functions based on manually designed criteria (Chen et al., 2018; Kendall et al., 2018),
 156 but these methods are often heuristic, ignore dynamic gradient interactions, and lack strong theore-
 157 matical foundations. Gradient manipulation methods (Sener & Koltun, 2018; Yu et al., 2020; Liu et al.,
 158 2021b;a; 2023) instead combine gradients from different tasks at each step. For example, Sener
 159 & Koltun (2018) uses an upper bound for efficiency, Yu et al. (2020) projects gradients to avoid
 160 conflicts, Liu et al. (2021b;a) provide a closed-form solution minimizing average loss, and Liu et al.
 161 (2023) introduces a fast dynamic weighting method. Although MOO is explored in multi-task learn-
 162 ing, DTO-KD uniquely applies it to knowledge distillation, formulating it as a dynamic trade-off
 163 optimization problem to resolve conflicts between task and distillation objectives.

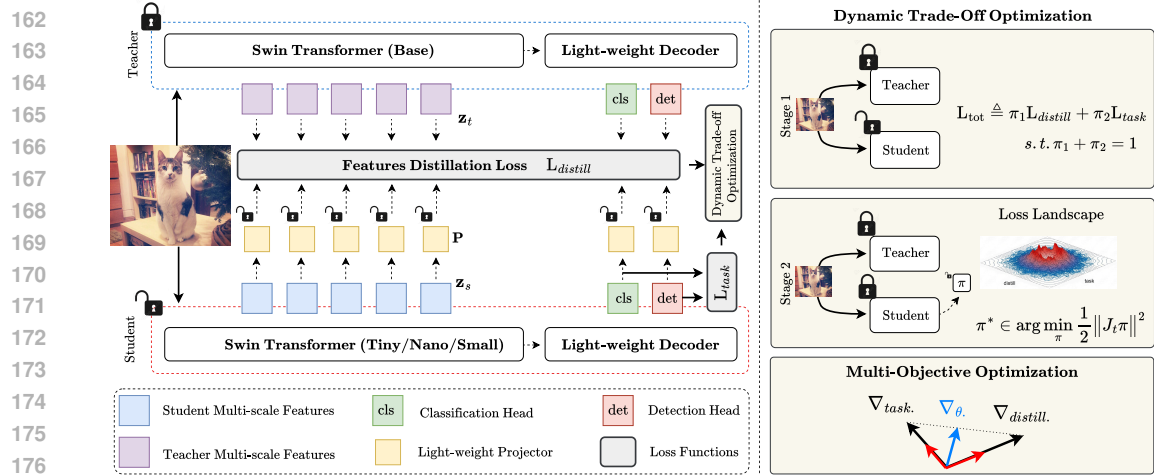


Figure 2: In DTO-KD, the teacher and student models simultaneously process the input image \mathbf{x} . Each network consists of a Swin Transformer with a lightweight decoder. The teacher’s features (\mathbf{z}_t), and the student’s (\mathbf{z}_s), are aligned using multiple lightweight projectors (\mathbf{P}) at different scales. We formulate training as a multi-objective optimization (MOO) problem and propose a Dynamic Trade-off Optimization module that jointly minimizes the distillation loss $\mathbf{L}_{\text{distill}}$ and the task-specific loss \mathbf{L}_{task} , guiding them toward Pareto optimality.

3 METHOD

We introduce a Dynamic Trade-off Optimization for Knowledge Distillation (DTO-KD), with a specific focus on resolving the conflicting objectives in the KD process.

Problem formulation. We aim to transfer knowledge from a high-capacity teacher model with parameters ϕ , to a more compact model student, with parameters θ , focusing mainly on classification and detection tasks in visual recognition. We show the training data with $\mathcal{S} = \{(\mathbf{x}_i, \mathbf{y}_i)\}_{i=1}^N$, with $\mathbf{x}_i \in \mathbb{R}^d$ being the i -th input instance and \mathbf{y}_i the corresponding target (e.g. a class label, bounding box). Our goal is to train the student model to effectively mimic the behavior of the teacher model over the dataset \mathcal{S} . Figure 2 shows an illustration of our proposed framework.

Effectively performing knowledge distillation requires balancing two objectives: the student must learn from two supervisory signals (e.g., one from the teacher and one from the task). We represent the teacher’s loss as $\mathbf{L}_{\text{distill}}$ and the task’s loss as \mathbf{L}_{task} . While we will define these more specifically for image classification and object detection in the appendix, we provide their general forms here:

$$\mathbf{L}_{\text{distill}}(\theta) \triangleq \mathbb{E}_{(\mathbf{x}, \mathbf{y}) \sim \mathcal{S}} \ell_{\text{distill}}(f_s(\mathbf{x}; \theta), f_t(\mathbf{x}; \phi)) \quad (1)$$

$$\mathbf{L}_{\text{task}}(\theta) \triangleq \mathbb{E}_{(\mathbf{x}, \mathbf{y}) \sim \mathcal{S}} \ell_{\text{task}}(f_s(\mathbf{x}; \theta), f_t(\mathbf{x}; \phi)) \quad (2)$$

The conventional KD approaches (e.g., (Hu et al., 2024; Zheng & Yang, 2024)) train the student model by optimizing the loss as

$$\mathbf{L}_{\text{tot}}(\theta) \triangleq \alpha_1 \mathbf{L}_{\text{distill}}(\theta) + \alpha_2 \mathbf{L}_{\text{task}}(\theta), \quad (3)$$

where $\alpha_1, \alpha_2 \in \mathbb{R}_+$ are the combination weights and hyperparameters of the model. The gradient of $\mathbf{L}_{\text{tot}}(\theta)$ is

$$\mathbf{g}_{\text{tot}} = \nabla \mathbf{L}_{\text{tot}}(\theta) = \alpha_1 \mathbf{g}_{\text{dist}} + \alpha_2 \mathbf{g}_{\text{task}} \quad (4)$$

where $\mathbf{g}_{\text{dist}} = \nabla \mathbf{L}_{\text{distill}}(\theta)$ and $\mathbf{g}_{\text{task}} = \nabla \mathbf{L}_{\text{task}}(\theta)$ are the gradients of the distillation and task losses, respectively. Minimizing loss in Equation (3) for joint training introduces the following challenges:

Gradient Conflict (GrC). This occurs when the gradients of the distillation loss and the task loss conflict with each other. Mathematically, GrC happens when $\langle \mathbf{g}_{\text{dist}}, \mathbf{g}_{\text{task}} \rangle < 0$. During the optimization of the total loss $\mathbf{L}_{\text{tot}}(\theta)$, the occurrence of GrC leads to conflicting gradient updates. Specifically, the total gradient \mathbf{g}_{tot} may contradict either \mathbf{g}_{dist} or \mathbf{g}_{task} , causing detrimental effects on one or both objectives. This conflict can exacerbate the learning dynamics, particularly in complex vision tasks such as object detection, by introducing unnecessary complexity into the training process.

Gradient Dominance (GrD). It arises when the gradients have significantly different magnitudes, leading one to dominate the update. When minimizing $L_{\text{tot}}(\theta)$, this imbalance may cause one objective to be completely neglected, as the update direction is primarily determined by the larger gradient, which can be estimated as $\frac{\|\mathbf{g}_{\text{dist}}\|}{\|\mathbf{g}_{\text{task}}\|}$. Lastly, tuning the hyperparameters α_1 and α_2 might become extremely tricky as the norm of gradients varies throughout optimization.

To address the aforementioned challenges, we advocate for the use of multi-objective optimization in KD. Specifically, we formulate the training process as optimizing the objective vector $\mathbf{L}_{\text{tot}}(\theta) = (L_{\text{distill}}(\theta), L_{\text{task}}(\theta))^{\top}$. The goal is to find a solution θ^* on the Pareto front, *i.e.*, a solution that is not dominated by any other parameter vector $\tilde{\theta}$. Formally, θ^* is Pareto optimal if is no $\tilde{\theta}$ such that

$$\begin{pmatrix} L_{\text{distill}}(\tilde{\theta}) \\ L_{\text{task}}(\tilde{\theta}) \end{pmatrix} \preceq \begin{pmatrix} L_{\text{distill}}(\theta^*) \\ L_{\text{task}}(\theta^*) \end{pmatrix} \quad (5)$$

The notation $\mathbf{a} \preceq \mathbf{b}$ here means that vector \mathbf{a} achieves a lower value for all its elements simultaneously over \mathbf{b} . As we will discuss in the next section, formulating KD using the proposed algorithm addresses both GrC and GrD by aligning the gradients. Furthermore, the use of MOO mitigates the difficulty of hyperparameter tuning, as it eliminates the need to manually define α_1 and α_2 .

3.1 KD AS A DYNAMIC TRADE-OFF OPTIMIZATION

Inspired by Liu et al. (2023), we followed a two stage approach for learning the optimal trade-off between conflicting objectives during the model training.

Stage 1: In stage 1 and at time t , we update the student model via $\theta_{t+1} = \theta_t - \eta \mathbf{g}_t$, where $\eta \in \mathbb{R}_+$ is the learning step size. We define the rate of improvement for the distillation and task losses as:

$$\begin{aligned} r_{\text{dist}}(\mathbf{g}_t) &= \frac{L_{\text{distill}}(\theta_t) - L_{\text{distill}}(\theta_{t+1})}{L_{\text{distill}}(\theta_t)}, \\ r_{\text{task}}(\mathbf{g}_t) &= \frac{L_{\text{task}}(\theta_t) - L_{\text{task}}(\theta_{t+1})}{L_{\text{task}}(\theta_t)}. \end{aligned} \quad (6)$$

In essence, $r_{\text{dist}}(\mathbf{g}_t)$ and $r_{\text{task}}(\mathbf{g}_t)$ measure how much each loss can be improved by moving the parameters with $-\eta \mathbf{g}_t$. A larger value of r_{dist} or r_{task} implies the associated task has been improved more.

Stage 2: In stage 2, our goal is to determine an update \mathbf{g}_t that maximizes the improvement over the worst-case rate. This can be achieved using a min-max optimization as:

$$\max_{\mathbf{g}_t \in \mathbb{R}^n} \min_{i \in \{\text{dist, task}\}} \frac{1}{\gamma} r_i(\mathbf{g}_t) - \frac{1}{2} \|\mathbf{g}_t\|^2. \quad (7)$$

Here, $\gamma \in \mathbb{R}_+$ is a weighting hyperparameter. As shown in Liu et al. (2023), the solution of Equation (7) can be obtained via solving its dual problem as (see proposition 3.1 in Liu et al. (2023)). Define $\boldsymbol{\pi} = (\pi_1, \pi_2)^{\top}$ on the simplex Δ (*i.e.*, $\pi_1 + \pi_2 = 1$, $\pi_1, \pi_2 \geq 0$), and let $\mathbf{J}_t \in \mathbb{R}^{n \times 2}$ be

$$\mathbf{J}_t = [\nabla \log(L_{\text{distill}}(\theta_t)) \mid \nabla \log(L_{\text{task}}(\theta_t))]^{\top} \quad (8)$$

Then

$$\boldsymbol{\pi}_t^* \in \arg \min_{\boldsymbol{\pi} \in \Delta} \frac{1}{2} \|\mathbf{J}_t \boldsymbol{\pi}\|^2, \quad (9)$$

and $\mathbf{g}_t = \mathbf{J}_t \boldsymbol{\pi}^* = \pi_1 \nabla \log(L_{\text{distill}}(\theta_t)) + \pi_2 \nabla \log(L_{\text{task}}(\theta_t))$.

Theoretical Properties. The problem formulation in Equation (9) admits an analytical solution, unlike the general case studied in Liu et al. (2023). In this part, we establish key theoretical properties of the obtained update direction \mathbf{g}^* .

Theorem 3.1 (Closed Form Solution). *Let $\mathbf{J}_t = [\nabla \log(L_{\text{distill}}(\theta_t)), \nabla \log(L_{\text{task}}(\theta_t))] \in \mathbb{R}^{n \times 2}$. The closed-form solution to the optimization problem*

$$\begin{aligned} \boldsymbol{\pi}^* &\in \arg \min_{\boldsymbol{\pi}} \frac{1}{2} \|\mathbf{J}_t \boldsymbol{\pi}\|^2 \\ \text{s.t.} \quad \pi_1 + \pi_2 &= 1 \end{aligned} \quad (10)$$

270 is given by

271
$$\pi_1^* = \frac{g_{22} - g_{12}}{g_{11} + g_{22} - 2g_{12}}, \quad (11)$$

272
$$\pi_2^* = \frac{g_{11} - g_{12}}{g_{11} + g_{22} - 2g_{12}}, \quad (12)$$

273 where $\mathbf{G} = \mathbf{J}_t^\top \mathbf{J}_t$ is the Gram matrix:

274
$$\mathbf{G} = \begin{bmatrix} g_{11} & g_{12} \\ g_{21} & g_{22} \end{bmatrix},$$

275 with elements

276
$$g_{11} = \|\nabla \log(L_{\text{distill}}(\boldsymbol{\theta}_t))\|^2, \quad (13)$$

277
$$g_{12} = g_{21} = \langle \nabla \log(L_{\text{distill}}(\boldsymbol{\theta}_t)), \nabla \log(L_{\text{task}}(\boldsymbol{\theta}_t)) \rangle, \quad (14)$$

278
$$g_{22} = \|\nabla \log(L_{\text{task}}(\boldsymbol{\theta}_t))\|^2. \quad (15)$$

280 The closed-form nature of this solution allows for efficient computation of the optimal weighting
281 factors. One key property of the derived solution is that the update direction aligns with both ob-
282 jectives, ensuring that both the distillation and task losses are reduced simultaneously. This directly
283 addresses GrC by preventing destructive interference between the two gradients.284 **Corollary 3.2** (Alignment of \mathbf{g}^*). Define $\mathbf{g}_1 = \nabla \log(L_{\text{distill}}(\boldsymbol{\theta}_t))$ and $\mathbf{g}_2 = \nabla \log(L_{\text{task}}(\boldsymbol{\theta}_t))$. Then
285 the update direction $\mathbf{g}^* = \pi_1 \mathbf{g}_1 + \pi_2 \mathbf{g}_2$ for π^* defined in 11 is aligned with both \mathbf{g}_1 and \mathbf{g}_2 .286 Another key property of the proposed solution is that it enforces equal contribution of the update
287 direction to both gradients, effectively addressing GrD.288 **Corollary 3.3** (Equal Contribution of \mathbf{g}^* to Both Losses). In Corollary 3.2, we showed that

289
$$\langle \mathbf{g}^*, \mathbf{g}_1 \rangle = \langle \mathbf{g}^*, \mathbf{g}_2 \rangle = \frac{g_{11}g_{22} - g_{12}^2}{\|\mathbf{g}_1 - \mathbf{g}_2\|^2}.$$

290 This implies that the update direction contributes equally to the descent of both the distillation and
291 task losses, effectively mitigating gradient dominance.292 An important aspect of any gradient-based optimization method is ensuring that update magnitudes
293 remain within a controlled range to prevent vanishing or exploding gradients. Our solution satisfies
294 both a lower and an upper bound on $\|\mathbf{g}^*\|$, ensuring stability during training.295 **Corollary 3.4** (Lower Bound on $\|\mathbf{g}^*\|$). The norm of the optimal update direction \mathbf{g}^* satisfies the
296 lower bound:

297
$$\|\mathbf{g}^*\| \geq \frac{1}{\sqrt{2}} \min(\|\mathbf{g}_1\|, \|\mathbf{g}_2\|). \quad (16)$$

300 This implies that the update magnitude remains controlled and does not collapse under gradient
301 imbalance.302 **Corollary 3.5** (Upper Bound on $\|\mathbf{g}^*\|$). The norm of the optimal update direction \mathbf{g}^* satisfies the
303 upper bound:

304
$$\|\mathbf{g}^*\| \leq \frac{\|\mathbf{g}_1\| \|\mathbf{g}_2\|}{\|\mathbf{g}_1\| - \|\mathbf{g}_2\|}. \quad (17)$$

305 As such, the magnitude of the updates does not grow excessively with different gradient scales.

306 Finally, we observe that the algorithm's convergence is ensured by the general theoretical frame-
307 work outlined in Liu et al. (2023). As our formulation aligns with it, the proposed optimization is
308 guaranteed to converge to a Pareto optimal front.309 **Practical Implementation.** The detailed algorithm for the proposed DTO-KD approach is de-
310 tailed in Algorithm 1. The distillation and task weights π are initialized to 0.5. The algorithm
311 begins by initializing the teacher as a frozen model and the student as a trainable model, and then
312 extracts latent features from both for each training batch. The *DistillHead* and *TaskHead* refer to
313 specific heads learning distillation and the task, respectively. It computes the distillation and task

324 **Algorithm 1** Dynamic Trade-off Optimisation for KD

```

325 1: Inputs: Dataset  $\mathcal{S} = \{(\mathbf{x}_i, \mathbf{y}_i), \dots\}$ ; Teacher  $f_t$ 
326 2: Initialise: Student  $f_s$  with  $\theta$ ; Task weight  $\pi_{distill} = \pi_{task} \leftarrow \frac{1}{2}$ 
327 3: for  $t = 1 : T$  do (iterations)
328 4:    $\mathbf{x}_\tau, \mathbf{y}_\tau = \{(\mathbf{x}_b, \mathbf{y}_b)\}_{b=1}^B \sim \mathcal{S}$  (batch)
329 5:    $\mathbf{z}_t, \mathbf{z}_s \leftarrow f_t(\mathbf{x}_\tau), f_s(\mathbf{x}_\tau)$  (latent features)
330 6:    $\hat{\mathbf{z}}_t, \hat{\mathbf{z}}_s \leftarrow \mathbf{z}_t^\top \mathbf{P} \mathbf{z}_s$  (projection)
331 7:    $\mathbf{L}(\boldsymbol{\theta}_t) = \begin{bmatrix} \mathbf{L}_{distill} \\ \mathbf{L}_{task} \end{bmatrix} = \begin{bmatrix} \ell_{distill}(DistillHead(\hat{\mathbf{z}}_s, \hat{\mathbf{z}}_t)) \\ \ell_{task}(TaskHead(\mathbf{z}_s), \mathbf{y}_\tau) \end{bmatrix}$  (loss vector)
332 8:    $\mathbf{g}_t = \pi_{distill} \nabla \log(\mathbf{L}_{distill}(\boldsymbol{\theta}_t)) + \pi_{task} \nabla \log(\mathbf{L}_{task}(\boldsymbol{\theta}_t))$ 
333 9:    $\boldsymbol{\theta}_{t+1} = \boldsymbol{\theta}_t - \gamma \mathbf{g}_t$  (student model learning)
334 10:   $\mathbf{L}(\boldsymbol{\theta}_{t+1}) \leftarrow f_s(\mathbf{x}_\tau)$  (frozen model inference)
335 11:   $\mathbf{r}(\mathbf{g}_t) = \begin{bmatrix} r_{distill}(\mathbf{g}_t) \\ r_{task}(\mathbf{g}_t) \end{bmatrix} = \begin{bmatrix} \frac{\mathbf{L}_{distill}(\boldsymbol{\theta}_t) - \mathbf{L}_{distill}(\boldsymbol{\theta}_{t+1})}{\mathbf{L}_{distill}(\boldsymbol{\theta}_t)} \\ \frac{\mathbf{L}_{task}(\boldsymbol{\theta}_t) - \mathbf{L}_{task}(\boldsymbol{\theta}_{t+1})}{\mathbf{L}_{task}(\boldsymbol{\theta}_t)} \end{bmatrix}$  (update direction)
336 12:   $\boldsymbol{\pi}(t+1) = \boldsymbol{\pi}(t) - \eta_\pi \nabla_{\boldsymbol{\pi}} \frac{1}{2} \left\| \pi_{distill}(t) \log(\mathbf{L}_{distill}(\boldsymbol{\theta}_t)) + \pi_{task}(t) \log(\mathbf{L}_{task}(\boldsymbol{\theta}_t)) \right\|^2$  (optimize task weights)
337
338
339
340
341
342
343
```

losses, combines their gradients according to the current task weights, and updates the student model accordingly. After each update, the task weights are recalculated in closed form based on the relative improvement of each loss, ensuring a balanced optimization that aligns both the distillation and task objectives. Despite having strong theoretical properties, MTL algorithms (Liu et al., 2023), including the one we have developed above, require access to per task gradient, in our case access to $\mathbf{J} = [\nabla \log(\mathbf{L}_{distill}(\boldsymbol{\theta}_t)), \nabla \log(\mathbf{L}_{task}(\boldsymbol{\theta}_t))]$. This incurs performing two backpropagation per iteration, which is not desired. Instead, one can advocate to amortizing the training. This leads to an approximation to the algorithm while ensuring that an extra backprop step is not required. In short, the parameters $\boldsymbol{\pi} = (\pi_{distill}, \pi_{task})$ are updated via

$$\boldsymbol{\pi}(t+1) = \boldsymbol{\pi}(t) - \eta_\pi \nabla_{\boldsymbol{\pi}} \frac{1}{2} \left\| \pi_{distill}(t) \log(\mathbf{L}_{distill}(\boldsymbol{\theta}_t)) + \pi_{task}(t) \log(\mathbf{L}_{task}(\boldsymbol{\theta}_t)) \right\|^2. \quad (18)$$

The update in Equation (18) does not guarantee $\boldsymbol{\pi} \in \Delta$, one should renormalize it via a softmax function. We have empirically observed that the amortized algorithm comfortably outperforms state-of-the-art KD algorithms with significant improvement over training speed. Specifically, the DTO-KD reaches the top performance of Roy Miles & Deng (2024) with 300 epochs in just 240 epochs.

4 EXPERIMENTS

We evaluate DTO-KD on two distinct vision tasks: image classification and object detection. For image classification, we adopt a CNN-based teacher model, RegNetY-160 (Radosavovic et al., 2020), and use transformer-based DeiT (Touvron et al., 2022) Small and Tiny as student models. For object detection, we employ transformer-based ViDT-Base (Song et al., 2021) as the teacher model, with ViDT-Small, ViDT-Tiny, and ViDT-Nano serving as the student models. Additionally, to assess the robustness of our method, we conduct distillation experiments using ViDT-Small as the teacher.

Implementation details: In DTO-KD, we reformulate model training as a gradient-based dynamic trade-off optimization problem. For the overall optimization across both classification and detection tasks, we use AdamW with a learning rate of 0.025 and a weight decay of 0.01. For classification, we adopt the training strategy and parameters from DeiT (Touvron et al., 2021a). Additionally, for data augmentation, we follow the method outlined in Roy Miles & Deng (2024). For learning, we employ AdamW (Loshchilov & Hutter, 2019) with a learning rate of 0.001 and a weight decay of 0.05. For object detection, we adhere to the training methodology from ViDT (Song et al., 2021). DTO-KD is trained using AdamW (Loshchilov & Hutter, 2019) with an initial learning rate of 10-4 for the body, neck, and head. We use the same hyperparameters as those in the ViDT (Song et al., 2021) transformer encoder and decoder. All experiments are conducted using PyTorch (Paszke et al., 2017) framework and executed on four NVIDIA H100 GPUs.

	Method	Venue	Top@1	Teacher	#Param.
378	RegNetY-160 (Radosavovic et al., 2020)	<i>CVPR20</i>	82.6	None	84M
379	CaiT-S24 (Touvron et al., 2021b)	<i>ICCV21</i>	83.4	None	47M
380	DeiT3-B (Touvron et al., 2022)	<i>ECCV22</i>	83.8	None	87M
381	DeiT-Ti (Touvron et al., 2021a)	<i>ICML21</i>	72.2	None	5M
382	DeiT-Ti (KD) (Touvron et al., 2021a)	<i>ICML21</i>	74.5	Regnety-160	6M
383	↳ 1000 epochs	<i>ICML21</i>	76.6	Regnety-160	6M
384	CivT-Ti (Ren et al., 2022)	<i>CVPR22</i>	74.9	Regnety-600m	6M
385	Manifold (Hao et al., 2022)	<i>NeurIPS22</i>	76.5	CaiT-S24	6M
386	DearKD (Chen et al., 2022)	<i>CVPR22</i>	74.8	Regnety-160	6M
387	↳ 1000 epochs	<i>CVPR22</i>	77.0	Regnety-160	6M
388	USKD (Yang et al., 2023)	<i>ICCV23</i>	75.0	Regnety-160	6M
389	MaskedKD (Son et al., 2024)	<i>ECCV24</i>	75.4	CaiT-S24	6M
390	SRD (Miles & Mikolajczyk, 2024)	<i>AAAI24</i>	77.2	Regnety-160	6M
391	V_k D-Ti (Roy Miles & Deng, 2024)	<i>CVPR24</i>	78.3	Regnety-160	6M
392	DTO-KD (Ti)		79.7	Regnety-160	6M
393	DeiT-S (Touvron et al., 2021a)	<i>ICML21</i>	79.8	None	22M
394	DeiT-S (KD) (Touvron et al., 2021a)	<i>ICML21</i>	81.2	Regnety-160	22M
395	↳ 1000 epochs	<i>ICML21</i>	82.6	Regnety-160	22M
396	CivT-S (Ren et al., 2022)	<i>CVPR22</i>	82.0	Regnety-4gf	22M
397	DearKD (Chen et al., 2022)	<i>CVPR22</i>	81.5	Regnety-160	22M
398	↳ 1000 epochs	<i>CVPR22</i>	82.8	Regnety-160	22M
399	USKD (Yang et al., 2023)	<i>ICCV23</i>	80.8	Regnety-160	22M
400	MaskedKD (Son et al., 2024)	<i>ECCV24</i>	81.4	Deit3-B	22M
401	SRD (Miles & Mikolajczyk, 2024)	<i>AAAI24</i>	82.1	Regnety-160	22M
402	V_k D-S (Roy Miles & Deng, 2024)	<i>CVPR24</i>	82.3	Regnety-160	22M
403	DTO-KD (S)		83.1	Regnety-160	22M

Table 1: **Object Classification task:** DTO-KD on the ImageNet-1K dataset. Unless specified, each model is only trained for 300 epochs.

4.1 OBJECT CLASSIFICATION USING IMAGENET-1K DATASET

We conducted extensive experiments on the ImageNet-1K dataset, using the RegNetY-160 (Radosavovic et al., 2020) model, pre-trained on the larger ImageNet-21K dataset, as the teacher to facilitate robust knowledge transfer. Two student models, DeiT-tiny and DeiT-small, were trained for 300 epochs on ImageNet-1K, and their performance was compared against existing state-of-the-art methods. As shown in Table 1, our approach demonstrates significant improvements in accuracy for both student models. Specifically, DTO-KD outperforms the baseline Touvron et al. (2021a) by 5.2 percentage points (pp) for the tiny model and 1.9 pp for the small model. Additionally, DeiT-tiny surpasses the previous state-of-the-art method Roy Miles & Deng (2024) by 1.4 pp, indicating a substantial enhancement in classification accuracy. For DeiT-small, our approach achieves a 0.8 pp accuracy improvement over Roy Miles & Deng (2024).

Additionally, compared to the baseline (Touvron et al., 2021a), which was trained for 1000 epochs, DTO-KD achieves a 3.1 percentage point (pp) improvement for the tiny model and a 0.5 pp improvement for the small model with just 300 epochs. This highlights the efficiency of our approach, demonstrating its ability to deliver competitive performance in significantly less training time, making it both effective and scalable.

4.2 OBJECT CLASSIFICATION USING CIFAR-100 DATASET

Conventional knowledge distillation methods are typically evaluated on both homogeneous and heterogeneous CNN architectures using the CIFAR-100 dataset. To position DTO-KD against these approaches, we benchmarked it following the protocols of prior KD works (Chen et al., 2021; Wang et al., 2024). Table 2 shows that DTO-KD also achieves superior results and reinforces its superiority, establishing a new SOTA by outperforming previous works in both small- and large-dataset settings.

4.3 OBJECT DETECTION

Table 3 demonstrates that our proposed method, DTO-KD, achieves state-of-the-art object detection performance on the MS-COCO benchmark (Lin et al., 2014), leveraging the ViDT transformer architecture (Song et al., 2022) for its strong performance and efficiency on consumer hardware. DTO-KD consistently improves upon various ViDT variants, enhancing the Swin-nano backbone

	Methods	Homogeneous			Heterogeneous			ResNet-32×4 ShuffleNet-V2
		ResNet-56 ResNet-20	WRN-40-2 WRN-40-1	ResNet-32×4 ResNet-8×4	ResNet-50 MobileNet-V2	ResNet-32×4 ShuffleNet-V1	ResNet-32×4 ShuffleNet-V2	
435	Teacher	72.34	75.61	79.42	79.34	79.42	79.42	
436	Student	69.06	71.98	72.50	64.60	70.50	71.82	
437	FitNet (Romero et al., 2015)	69.21	72.24	73.50	63.16	73.59	73.54	
438	RKD (Park et al., 2019)	69.61	72.22	71.90	64.43	72.28	73.21	
439	PKT (Passalis et al., 2020)	70.34	73.45	73.64	66.52	74.10	74.69	
440	KD (Hinton et al., 2015)	70.66	73.54	73.33	67.65	74.07	74.45	
441	OFD (Heo et al., 2019b)	70.98	74.33	74.95	69.04	75.98	76.82	
442	CRD (Tian et al., 2019)	71.16	74.14	75.51	69.11	75.11	75.65	
443	DIST (Huang et al., 2022)	71.78	74.42	75.79	69.17	75.23	76.08	
444	ReviewKD (Chen et al., 2021)	71.89	75.09	75.63	69.89	77.45	77.78	
445	DKD (Zhao et al., 2022b)	71.97	74.81	75.44	70.35	76.45	77.07	
446	ReviewKD++ (Wang et al., 2024)	72.05	75.66	76.07	70.45	77.68	77.93	
447	DTO-KD (ours)	72.29	75.70	76.34	70.87	77.92	78.11	

Table 2: **Object Classification task:** DTO-KD evaluated on both homogeneous and heterogeneous CNN architectures using the CIFAR-100 dataset.

		ViDT Model	Epochs	AP	AP ₅₀	AP ₇₅	AP _S	AP _M	AP _L	#Params	FPS
448	Teacher	Swin-base (Song et al., 2021)	50	49.4	69.6	53.4	31.6	52.4	66.8	0.1B	9.0
449		Swin-nano (Song et al., 2021)	50	40.4	59.6	43.3	23.2	42.5	55.8		
450		Token-Matching (Song et al., 2022)	50	41.9	61.2	44.7	23.6	44.1	58.7	16M	20.0
451		V _k D-nano (Roy Miles & Deng, 2024)	50	43.0	62.3	46.2	24.8	45.3	60.1		
452		DTO-KD (nano)	50	43.7	63.1	46.8	25.1	46.2	61.9		
453	Student	Swin-tiny (Song et al., 2021)	50	44.8	64.5	48.7	25.9	47.6	62.1		
454		Token-Matching (Song et al., 2022)	50	46.6	66.3	50.4	28.0	49.5	64.3	38M	17.2
455		V _k D-tiny (Roy Miles & Deng, 2024)	50	46.9	66.6	50.9	27.8	49.8	64.6		
456		DTO-KD (tiny)	50	47.4	67.2	51.3	28.0	50.7	65.8		
457		Swin-small (Song et al., 2021)	50	47.5	67.7	51.4	29.2	50.7	64.8		
458		Token-Matching (Song et al., 2022)	50	49.2	69.2	53.6	30.7	52.3	66.8	61M	12.1
459		V _k D-small (Roy Miles & Deng, 2024)	50	48.5	68.4	52.4	30.8	52.2	66.0		
460		DTO-KD (small)	50	49.6	69.4	53.9	31.6	53.1	67.1		

Table 3: **Object Detection task:** Comparison with other detectors on COCO, with student models distilled from a pre-trained ViDT-base. Note that DTO-KD consistently outperforms all challenging knowledge distillation baseline approaches.

by 0.7 percentage points (pp), Swin-tiny by 0.5pp, and Swin-small by 1.1pp. Notably, DTO-KD-small, with just 61M parameters, outperforms Swin-base (0.1B parameters) when both are trained from scratch. Additionally, DTO-KD-tiny, with 38M parameters, achieves nearly the same performance as Swin-small (61M parameters).

4.4 ABLATION STUDIES

Impact of different components in DTO-KD: We conduct a thorough evaluation of the impact of each primary component in DTO-KD, specifically assessing both stages of dynamic trade-off optimization, and post processing using gradient clipping. These components were introduced to enhance the knowledge distillation process, and their individual contributions are analyzed in Table 4. The results demonstrate that each stage significantly contributes to the performance of DTO-KD, with all showing a positive effect on the overall effectiveness of the model. Dynamic Trade-off opti-

Proj	Dynamic Trade-off Optimization	Grad. Clip	S:DTO-KD-nano / T:ViDT-base		
			AP	AP ₅₀	AP ₇₅
		✓	41.0	59.2	42.8
			41.8	61.2	44.7
479	✓		43.1	61.7	46.4
480	✓	✓	43.6	62.9	46.6
		✓	43.7	63.1	46.8

Table 4: **Component’s Impact Assessment:** An ablation study showing the impact of projector and optimisation. We also applied gradient clipping as a pre-processing step to both objectives to see its impact with and without DTO.

Teacher	Student		ViDT-nano		ViDT-tiny	
	ViDT (small)	ViDT (base)	ViDT (small)	ViDT (base)	ViDT (small)	ViDT (base)
No Distillation (Song et al., 2021)			40.4		44.8	
Token Matching (Song et al., 2022)	41.5	41.9	45.8	46.5		
V _k D (Roy Miles & Deng, 2024)	42.2	43.0	45.9	46.9		
DTO-KD (ours)	43.2	43.7	46.9	47.4		

Table 5: **Distillation from different teachers for the Object Detection task:** Comparison of ViDT on COCO2017 val set. We report AP for the student models distilled from different teacher models.

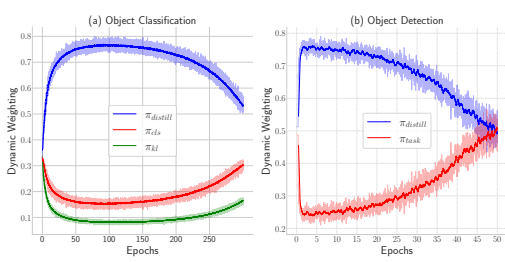


Figure 3: **Effectiveness of the Dynamic Balancing Strategy** on the object detection and the classification tasks.

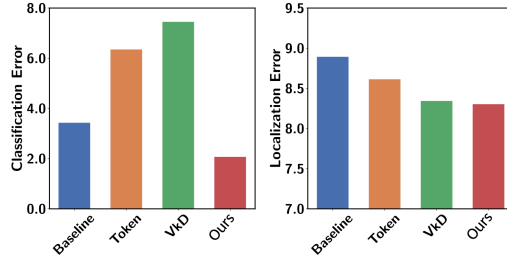


Figure 4: **Error analysis:** Our dynamic trade-off optimisation approach consistently lowers the classification and localisation errors.

mization enables the model to handle diverse objectives, and alignment between teacher and student models to facilitate smoother knowledge transfer.

Dynamic Balancing Strategy and π values: To better illustrate our approach, the figure below shows the varying weighting ratios of the distillation loss ($\pi_{distill}$) and the task losses (π_{task}) during training. As illustrated in **(a)**, we evaluate DTO-KD on a classification task using three distinct loss terms, demonstrating its ability to dynamically balance these objectives through adaptive weighting. In **(b)**, we extend this analysis to object detection with two loss terms, where DTO-KD’s gradient-based vector optimization initially prioritizes the distillation loss and progressively shifts focus toward the task-specific loss.

Subtask error analysis: We conduct a thorough analysis of both classification and localization errors (Bolya et al., 2020) in the object detection task. DTO-KD outperforms other methods, achieving fewer errors in both areas while maintaining a strong balance between them. Notably, other KD techniques (Roy Miles & Deng, 2024; Song et al., 2022) underperform in the classification subtask compared to the baseline (Song et al., 2021), highlighting the superior effectiveness of our approach. See Figure 4 for more details.

Distillation from different teachers: Table 5 demonstrates DTO-KD’s strong performance, even with smaller teachers like ViDT-small. This highlights its robustness, adaptability, and efficiency in resource-constrained settings, making it a versatile and effective distillation method across different teacher model scales.

5 LIMITATIONS

Like other KD methods, data availability is a bottleneck. DTO-KD is designed for distillation with available data, and extending it to data-free settings, especially for distilling from large pre-trained models, remains an open challenge. Extending DTO-KD to a data-free regime through sample synthesis may be more difficult due to its min-max optimization, which requires data for the training.

6 CONCLUSION

DTO-KD introduces a principled and effective solution to longstanding challenges in knowledge distillation, particularly for transformer-based architectures. By dynamically balancing task-specific and distillation objectives at the gradient level, DTO-KD mitigates supervision conflicts and gradient imbalances that arise from architectural mismatches between teacher and student models. This multi-objective formulation enables more stable and efficient training, resulting in student models that not only match but often exceed the performance of their non-distilled counterparts. Extensive evaluations on image classification and object detection benchmarks demonstrate that DTO-KD consistently achieves state-of-the-art results, setting a new standard for gradient-aware distillation methods. These improvements come with minimal computational overhead, making DTO-KD practical for real-world deployment.

540 REFERENCES
541

542 Daniel Bolya, Sean Foley, James Hays, and Judy Hoffman. Tide: A general toolbox for identifying
543 object detection errors. In *ECCV*, 2020.

544 Liqun Chen, Dong Wang, Zhe Gan, Jingjing Liu, Ricardo Henao, and Lawrence Carin. Wasserstein
545 Contrastive Representation Distillation. In *CVPR*, 2020.

546

547 Pengguang Chen, Shu Liu, Hengshuang Zhao, and Jiaya Jia. Distilling Knowledge via Knowledge
548 Review. In *CVPR*, 2021.

549

550 Xianing Chen, Qiong Cao, Yujie Zhong, Jing Zhang, Shenghua Gao, and Dacheng Tao. Dearkd:
551 Data-efficient early knowledge distillation for vision transformers. In *CVPR*, 2022.

552

553 Zhao Chen, Vijay Badrinarayanan, Chen-Yu Lee, and Andrew Rabinovich. GradNorm: Gradient
554 normalization for adaptive loss balancing in deep multitask networks. In Jennifer Dy and Andreas
555 Krause (eds.), *ICML*, 2018. URL <https://proceedings.mlr.press/v80/chen18a.html>.

556

557 Pengguang Chen et al. Distilling knowledge via knowledge review. In *CVPR*, 2021.

558

559 Mengya Gao, Yujun Shen, Quanquan Li, Junjie Yan, Liang Wan, Dahu Lin, Chen Change Loy, and
560 Xiaou Tang. An Embarrassingly Simple Approach for Knowledge Distillation. *arXiv*, 2018.

561

562 Zhiwei Hao, Jianyuan Guo, Ding Jia, Kai Han, Yehui Tang, Chao Zhang, Han Hu, and Yunhe Wang.
563 Learning efficient vision transformers via fine-grained manifold distillation. In *NeurIPS*, 2022.

564

565 Byeongho Heo, Jeesoo Kim, Sangdoo Yun, Hyojin Park, Nojun Kwak, and Jin Young Choi. A
566 comprehensive overhaul of feature distillation. In *ICCV*, 2019a.

567

568 Byeongho Heo, Jeesoo Kim, Sangdoo Yun, Hyojin Park, Nojun Kwak, and Jin Young Choi. A
569 comprehensive overhaul of feature distillation. In *Proceedings of the IEEE/CVF international
570 conference on computer vision*, pp. 1921–1930, 2019b.

571

572 Geoffrey Hinton, Oriol Vinyals, and Jeff Dean. Distilling the Knowledge in a Neural Network. In
573 *NeurIPS*, 2015.

574

575 Chengming Hu, Haolun Wu, Xuan Li, Chen Ma, Xi Chen, Jun Yan, Boyu Wang, and Xue Liu. Less
576 or more from teacher: Exploiting trilateral geometry for knowledge distillation. In *ICLR*, 2024.

577

578 Tao Huang, Shan You, Fei Wang, Chen Qian, and Chang Xu. Knowledge distillation from a stronger
579 teacher, 2022.

580

581 Tao Huang, Yuan Zhang, Mingkai Zheng, Shan You, Fei Wang, Chen Qian, and Chang Xu. Knowl-
582 edge diffusion for distillation. In *NeurIPS*, 2024.

583

584 Alex Kendall, Yarin Gal, and Roberto Cipolla. Multi-task learning using uncertainty to weigh losses
585 for scene geometry and semantics. In *CVPR*, 2018.

586

587 Jiguan Lin. Multiple-objective problems: Pareto-optimal solutions by method of proper equality
588 constraints. *IEEE Transactions on Automatic Control*, 1976.

589

590 Tsung Yi Lin, Michael Maire, Serge Belongie, James Hays, Pietro Perona, Deva Ramanan, Piotr
591 Dollár, and C. Lawrence Zitnick. Microsoft COCO: Common objects in context. In *ECCV*, 2014.

592

593 Bo Liu, Xingchao Liu, Xiaojie Jin, Peter Stone, and Qiang Liu. Conflict-averse gradient descent for
594 multi-task learning. In *NeurIPS*, 2021a.

595

596 Bo Liu, Yihao Feng, Peter Stone, and Qiang Liu. Famo: Fast adaptive mul-
597 titask optimization. In A. Oh, T. Naumann, A. Globerson, K. Saenko,
598 M. Hardt, and S. Levine (eds.), *NeurIPS*. Curran Associates, Inc., 2023. URL
599 https://proceedings.neurips.cc/paper_files/paper/2023/file/b2fe1ee8d936ac08dd26f2ff58986c8f-Paper-Conference.pdf.

594 Liyang Liu, Yi Li, Zhanghui Kuang, J Xue, Yimin Chen, Wenming Yang, Qingmin Liao, and Wayne
 595 Zhang. Towards impartial multi-task learning. In *ICLR*, 2021b.

596

597 Ilya Loshchilov and Frank Hutter. Decoupled weight decay regularization. In *ICLR*, 2019.

598

599 Roy Miles and Krystian Mikolajczyk. Understanding the role of the projector in knowledge distil-
 600 lation. In *AAAI*, 2024.

601

602 Seyed-Iman Mirzadeh, Mehrdad Farajtabar, Ang Li, and Hassan Ghasemzadeh. Improved Knowl-
 603 edge Distillation via Teacher Assistant: Bridging the Gap Between Student and Teacher. In *AAAI*,
 2020.

604

605 Wonpyo Park, Dongju Kim, Yan Lu, and Minsu Cho. Relational knowledge distillation. In *Proceed-
 606 ings of the IEEE/CVF conference on computer vision and pattern recognition*, pp. 3967–3976,
 607 2019.

608

609 Nikolaos Passalis, Maria Tzelepi, and Anastasios Tefas. Probabilistic knowledge transfer for
 610 lightweight deep representation learning. *IEEE Transactions on Neural Networks and Learning
 Systems*, 32(5):2030–2039, 2020.

611

612 Adam Paszke, Sam Gross, Soumith Chintala, Gregory Chanan, Edward Yang, Zachary DeVito,
 613 Zeming Lin, Alban Desmaison, Luca Antiga, and Adam Lerer. Automatic differentiation in
 614 pytorch. In *NeurIPS*, 2017.

615

616 Zengyu Qiu, Xinzhu Ma, Kunlin Yang, Chunya Liu, Jun Hou, Shuai Yi, and Wanli Ouyang. Better
 617 teacher better student: Dynamic prior knowledge for knowledge distillation. In *ICLR*, 2023.

618

619 Ilija Radosavovic, Raj Prateek Kosaraju, Ross Girshick, Kaiming He, and Piotr Dollár. Designing
 620 Network Design Spaces. In *CVPR*, 3 2020.

621

622 Sucheng Ren, Zhengqi Gao, Tianyu Hua, Zihui Xue, Yonglong Tian, Shengfeng He, and Hang Zhao.
 623 Co-advise: Cross Inductive Bias Distillation. In *CVPR*, 2022.

624

625 Adriana Romero, Nicolas Ballas, Samira Ebrahimi Kahou, Antoine Chassang, Carlo Gatta, and
 626 Yoshua Bengio. FitNets: Hints For Thin Deep Nets. In *ICLR*, 2015.

627

628 Ismail Elezi Roy Miles and Jiankang Deng. Vkd : Improving knowledge distillation using orthogo-
 629 nal projections. In *CVPR*, March 2024.

630

631 Ozan Sener and Vladlen Koltun. Multi-task learning as multi-objective optimization. In
 632 S. Bengio, H. Wallach, H. Larochelle, K. Grauman, N. Cesa-Bianchi, and R. Garnett (eds.),
 633 *NeurIPS*, 2018. URL https://proceedings.neurips.cc/paper_files/paper/2018/file/432aca3a1e345e339f35a30c8f65edce-Paper.pdf.

634

635 Seungwoo Son, Namhoon Lee, and Jaeho Lee. Maskedkd: Efficient distillation of vision transfor-
 636 mers with masked images. In *ECCV*, 2024.

637

638 Hwanjun Song, Deqing Sun, Sanghyuk Chun, Varun Jampani, Dongyoon Han, Byeongho Heo,
 639 Wonjae Kim, and Ming-Hsuan Yang. Vidt: An efficient and effective fully transformer-based
 640 object detector. In *ICLR*, 2021.

641

642 Hwanjun Song, Deqing Sun, Sanghyuk Chun, Varun Jampani, Dongyoon Han, Byeongho Heo,
 643 Wonjae Kim, and Ming-Hsuan Yang. Vidt: An efficient and effective fully transformer-based
 644 object detector. In *ICLR*, 2022.

645

646 Yonglong Tian, Dilip Krishnan, and Phillip Isola. Contrastive representation distillation. *arXiv
 preprint arXiv:1910.10699*, 2019.

647

648 Hugo Touvron, Matthieu Cord, Matthijs Douze, Francisco Massa, Alexandre Sablayrolles, and
 649 Hervé Jégou. Training data-efficient image transformers & distillation through attention. In
 650 *PMLR*, 2021a.

651

652 Hugo Touvron, Matthieu Cord, Alexandre Sablayrolles, Gabriel Synnaeve, and Hervé Jégou. Going
 653 deeper with image transformers. In *ICCV*, 2021b.

648 Hugo Touvron, Matthieu Cord, and Hervé Jégou. Deit iii: Revenge of the vit. In *ECCV*, 2022.
 649

650 Bichen Wang, Yuzhe Zi, Yixin Sun, Yanyan Zhao, and Bing Qin. Balancing forget quality and
 651 model utility: A reverse kl-divergence knowledge distillation approach for better unlearning in
 652 llms. In *Proceedings of the 2025 Conference of the North American Chapter of the Associa-
 653 tion for Computational Linguistics (NAACL 2025, Long Papers)*, pp. 1306–1321. Association for
 654 Computational Linguistics, 2025a. doi: 10.18653/v1/2025.nacllong.60.

655 Guanghui Wang, Zhiyong Yang, Zitai Wang, Shi Wang, Qianqian Xu, and Qingming Huang. Abkd:
 656 Pursuing a proper allocation of the probability mass in knowledge distillation via α - β -divergence.
 657 In Aarti Singh, Maryam Fazel, Daniel Hsu, Simon Lacoste-Julien, Felix Berkenkamp, Tegan
 658 Maharaj, Kiri Wagstaff, and Jerry Zhu (eds.), *Proceedings of the 42nd International Conference
 659 on Machine Learning (ICML 2025)*, volume 267 of *Proceedings of Machine Learning Research*,
 660 pp. 65167–65212. PMLR, Jul 2025b. URL <https://proceedings.mlr.press/v267/wang25dz.html>.

661

662 Jiabao Wang, Yuming Chen, Zhaohui Zheng, Xiang Li, Ming-Ming Cheng, and Qibin Hou. Crosskd:
 663 Cross-head knowledge distillation for object detection. In *CVPR*, 2024.

664 Yuzhu Wang et al. Improving knowledge distillation via regularizing feature direction and norm.
 665 In Aleš Leonardis, Elisa Ricci, Stefan Roth, Olga Russakovsky, Torsten Sattler, and Gü̈l Varol
 666 (eds.), *ECCV*, 2024.

667 Yuqiao Wen, Zichao Li, Wenyu Du, and Lili Mou. f-divergence minimization for sequence-
 668 level knowledge distillation. In *Proceedings of the 61st Annual Meeting of the Association
 669 for Computational Linguistics (Volume 1: Long Papers)*, pp. 10817–10834, Toronto, Canada,
 670 2023. Association for Computational Linguistics. doi: 10.18653/v1/2023.acl-long.605. URL
 671 <https://aclanthology.org/2023.acl-long.605/>.

672 Guodong Xu, Ziwei Liu, Xiaoxiao Li, and Chen Change Loy. Knowledge distillation meets self-
 673 supervision. *ECCV*, 2020.

674

675 Chuanguang Yang, Zhulin An, Linhang Cai, and Yongjun Xu. Hierarchical self-supervised aug-
 676 mented knowledge distillation. In *Proceedings of the Thirtieth International Joint Conference on
 677 Artificial Intelligence (IJCAI)*, pp. 1217–1223, 2021.

678 Zhendong Yang, Ailing Zeng, Zhe Li, Tianke Zhang, Chun Yuan, and Yu Li. From knowledge dis-
 679 tillation to self-knowledge distillation: A unified approach with normalized loss and customized
 680 soft labels. In *ICCV*, 2023.

681 Junho Yim. A Gift from Knowledge Distillation: Fast Optimization, Network Minimization and
 682 Transfer Learning. In *CVPR*, 2017.

683

684 Tianhe Yu, Saurabh Kumar, Abhishek Gupta, Sergey Levine, Karol Hausman, and
 685 Chelsea Finn. Gradient surgery for multi-task learning. In H. Larochelle, M. Ran-
 686 zato, R. Hadsell, M.F. Balcan, and H. Lin (eds.), *NeurIPS*, volume 33, 2020. URL
 687 https://proceedings.neurips.cc/paper_files/paper/2020/file/3fe78a8acf5fda99de95303940a2420c-Paper.pdf.

688

689 Ying Zhang, Tao Xiang, Timothy M. Hospedales, and Huchuan Lu. Deep Mutual Learning. In
 690 *CVPR*, 2018.

691 Borui Zhao, Quan Cui, Renjie Song, Yiyu Qiu, and Jiajun Liang. Decoupled knowledge distillation.
 692 In *CVPR*, 2022a.

693 Borui Zhao, Quan Cui, Renjie Song, Yiyu Qiu, and Jiajun Liang. Decoupled knowledge distillation.
 694 In *Proceedings of the IEEE/CVF Conference on computer vision and pattern recognition*, pp.
 695 11953–11962, 2022b.

696

697 Kaixiang Zheng and En-Hui Yang. Knowledge distillation based on transformed teacher matching.
 698 In *The Twelfth International Conference on Learning Representations (ICLR 2024)*, 2024. URL
 699 <https://openreview.net/pdf?id=MJ3K7uDGG1>.

700 Zaida Zhou, Chaoran Zhuge, Xinwei Guan, and Wen Liu. Channel Distillation: Channel-Wise At-
 701 tention for Knowledge Distillation. In *ICCV*, 2020. URL <http://arxiv.org/abs/2006.01683>.